ScienceDirect

Mendeleev Commun., 2015, **25**, 142–144

Mendeleev
Communications

Self-assembling of tapered benzenesulfonate-based dendrons with bulky aromatic focal groups

Maxim A. Shcherbina,*[a,b] Artem V. Bakirov,[a,b] Linglong Yan,[c] Uwe Beginn,[c]
Xiaomin Zhu,[d] Martin Möller[d] and Sergey N. Chvalun[a,b]

[a] *N. S. Enikolopov Institute of Synthetic Polymer Materials, Russian Academy of Sciences, 117393 Moscow, Russian Federation. Fax: +7 495 718 3404; e-mail: shcherbina@ispm.ru*
[b] *National Research Centre 'Kurchatov Institute', 123098 Moscow, Russian Federation*
[c] *Organic Materials Chemistry, Institute for Chemistry of New Materials, University of Osnabrück, D-49069 Osnabrück, Germany*
[d] *Institute of Technical and Macromolecular Chemistry, RWTH Aachen and DWI e.V., D-52056 Aachen, Germany*

DOI: 10.1016/j.mencom.2015.03.023

Comparative analysis of the structure and phase behavior of the synthesized compounds on the basis of symmetrically and asymmetrically substituted benzenesulfonic acids with bulky aromatic focal groups revealed that their phase behavior is determined equally by the shape of the mesogenic groups as well as by specific interactions at the focal points of the monodendrons.

Exploiting the self-assembly of amphiphilic conic and tapered dendrons for the rational design of functional supramolecular ensembles is an important area of modern materials science. Substantial interest in this field is caused by a wide variety of lyotropic and thermotropic mesophases as observed in systems with one-dimensional (smectic layers and bilayers), two-dimensional (ordered and disordered columnar phase) and three-dimensional (crystalline hexagonal and plastic crystals of different groups of symmetry and bicontinuous cubic lattices[1–7]) long range order. Despite of the apparent complexity of the observed phase behavior of tapered and cone-shaped dendrons, theoretical models developed so far allow one to explain the self-assembling of supramolecular aggregates and mesophases.

First, a geometrical approach should be mentioned: the volume radial distribution $\mathrm{d}V/\mathrm{d}r$[8] of Voronoi polyhedrons constructed for a crystal lattice of a particular group of symmetry is considered. The shape of the $\mathrm{d}V/\mathrm{d}r$ curve coincides with the cross-section of a dendron; *i.e.*, its projection on the plane perpendicular to its axis, fitting in a best way to the considered crystal lattice with minimal steric hindrances. Variations in temperature, pressure, humidity, solution acidity, *etc*. differently affect various parts of a molecule[9–11] leading to essential changes in dendron shape and, consequently, to a phase transition in the material. Moreover, the theory of microphase segregation developed for block copolymers in the limiting cases of weak[12] and strong[13] segregation is also applicable to amphiphilic dendrons: any repulsion of incompatible fragments is followed by their micro-segregation under simultaneous minimization of the interphase area. A general model incorporating two extreme cases was described,[14] considering not only the enthalpy of segregation but also its entropy, a tendency of the system to uniform space filling.

The synthesis of vast libraries of similar compounds with incrementally varied parameters makes it possible to analyze systematically the structure and phase behavior of amphiphilic compounds and their self-assembling.[15–18] Our recent studies of the alkali metal salts of 2,3,4-tris(dodecyloxy)benzenesulfonic acid[19,20] revealed that a modification in the shape of the mesogenic group due to variations in the size of its metal cation leads to predictable changes in the phase behavior. Conic dendrons with a small ion focal point tend to form smectic bilayers. With increasing temperature, these bilayers transform to spherical micelles packed into cubic lattices. With the bulky cations, the shape of the dendron resembles a truncated cone. In such mesogenes called cunitic (lat. *cuneus* = wedge) amphiphiles,[18] ordered and disordered columnar mesophases appear to be more stable.

Based on the experimental data, we concluded that the interaction of ionic pairs in the centers of supramolecular units defines the structure of the formed supramers. For this reason the compounds on the basis of benzenesulfonic acid possessing large focal groups, which are capable of specific interactions with an interaction energy comparable to that of ionic forces, such as π–π stacking, are of special interest. We studied the structure and temperature behavior of supramolecular aggregates formed by pyridinium 2,3,4-tris(dodecyloxy)benzenesulfonate **1**[†] and symmetrically substituted sodium and pyridinium *p*-{(*E*)-*p*-[3,4,5-tris(dodecyloxy)benzoyloxy]phenylazo}benzenesulfonates **2** and **3**, respectively, by wide- and small-angle X-ray diffraction, differential scanning calorimetry (DSC), polarizing optical microscopy (TPOM) and molecular modeling. Note that the intro-

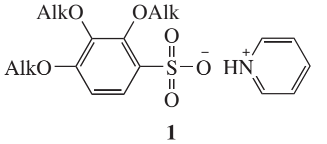

1

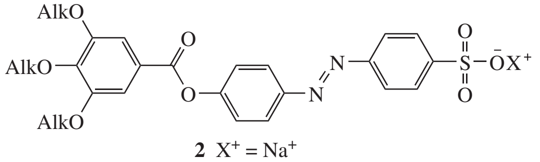

2 $X^+ = Na^+$
3 X^+ = pyridinium Alk = $C_{12}H_{25}$

[†] 2,3,4-Tris(dodecyloxy)benzenesulfonate **1** was obtained by the sulfonation of 1,2,3-tris(dodecyloxy)benzene [synthesized in 76% yield by the alkylation of pyrogallol (1,2,3-trihydroxybenzene) with 1-bromodecane in DMF, followed by recrystallization from acetone] with concentrated sulfuric acid at room temperature for 2 h. The following recrystallization from *n*-hexane provided 2,3,4-tris(dodecyloxy)benzenesulfonic acid in 87% yield. Then it was dissolved in pyridine by intense stirring for 24 h under a nitrogen atmosphere. The samples were subsequently dried in a rotary evaporator, recrystallized from methanol and dried *in vacuo* at 40 °C. The yield of compound **1** was no less than 98%.[18]

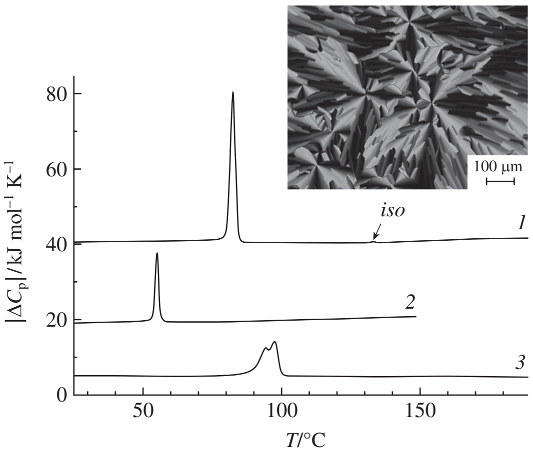

Figure 1 DSC heating scans of compounds (*1*) **1**, (*2*) **2** and (*3*) **3**. For clarity, curves for **1** and **2** are shifted along the vertical axis. The insert is a polarizing optical micrograph of compound **1** at 100 °C. The arrow marks the isotropization peak of compound **1**.

Table 1 Thermal transitions of compounds **1**–**3**.[a]

Compound	T_{meso}/°C	ΔH_{meso}/kJ mol^{-1}	T_{iso}/°C	ΔH_{iso}/kJ mol^{-1}
1	82	101	129	1.5
2	55	34	—[b]	—
3	95	68	200	< 0.5

[a] Subscripts ‘meso’ refer to the transition in a high-temperature mesophase, while subscripts ‘iso’ refer to the isotropization. [b] Isotropization was not observed up to 300 °C.

duction of an *E*/*Z*-photoisomerable azobenzene group into the structure of a dendron can open a new way of controlling the structure of supramolecular ensembles by means of light.[21–23]

It is important to note that the electrophilic aromatic substitution always leads to the sulfonation of 1,2,3-tris(dodecyloxy)benzene in the 4- and 6-positions of the benzene ring. Hence, the synthesis of compounds **2** and **3** based on the symmetrically substituted 3,4,5-tris(dodecyloxy)benzoic acid was performed as described in detail elsewhere.[24] The synthesized materials were white disperse crystalline powders, which became waxy on heating. The DSC scans of all the compounds are characterized by a strong endothermal effect which was attributed to an order–disorder mesomorphic transition according to the X-ray data. Transition temperatures and enthalpies measured by DSC (Figure 1) are given in Table 1. The transitions of both compounds **1** and **3** to an isotropic state are characterized by an extremely low heat effect testifying the low degree of an order of their high-temperature mesophases (see below). In case of compound **2**, an isotropization was not observed up to $T = 300$ °C when the samples started to decompose.

Figure 2 shows the temperature evolution of small-angle X-ray patterns of compound **1**. At room temperature, at least six orders of the smectic reflection are observed. The measured layer thickness was $d_{\mathrm{L}} = 42.7$ Å, while the length of the molecule with completely extended aliphatic tails calculated from molecular modeling was 22.5 Å. Thus, the bilayer structure of smectic mesophase can be concluded. The results of the molecular modeling of the layer structure of compound **1** (Figure 3) show that mutual arrangement and local order formation of the mesogenic groups are facilitated by the π–π-stacking interaction of the pyridinium fragments. On heating to 80 °C, this ordering is improved: the small-angle reflections become narrower and shift to the wide-angle region ($d_{\mathrm{L}} = 42.4$ Å). Two orders of the new reflection corresponding to the interplanar distance of $d = 30.6$ Å also developed.

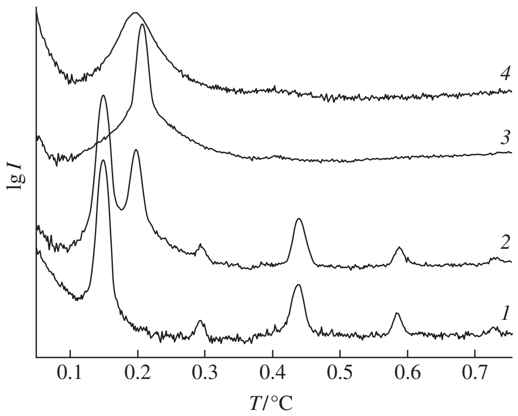

Figure 2 Small-angle X-ray scattering patterns of compound **1** at (*1*) room temperature, at (*2*) 80, (*3*) 110 and (*4*) 130 °C.

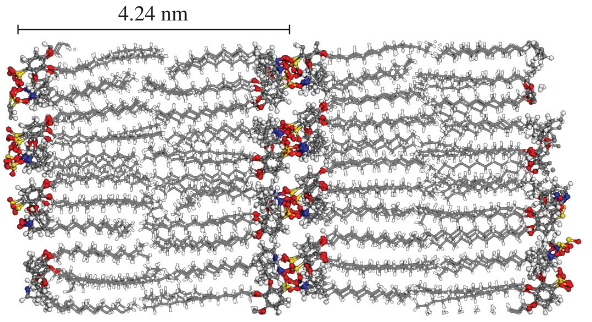

Figure 3 Molecular modeling of a smectic bilayer formed by **1**. Atomic sizes are estimated from van der Waals potentials.

The intensities of the reflections of the low-temperature smectic mesophase fall sharply on further heating, disappearing completely at 110 °C. Note that the characteristic fan-shaped texture of the samples observed in polarized light (Figure 1) changed insignificantly up to sample isotropization. Therefore, one can assume that a smectic–smectic transition occurs at 85 °C. As its heat effect is high, a high degree of ordering in the low-temperature phase can be expected. The isotropization taking place at 129 °C is characterized by a low heat of transition, as the ordering of a high-temperature smectic mesophase is poor. Isotropization of compound **1** is observed at 129 °C, while its decomposition starts at 150 °C, accompanied by the emission of gaseous products. However, the phase transitions of compound **1** are reversible at temperatures up to 150 °C.

The extension of the focal groups of mesogenic groups due to the introduction of azobenzene units (compounds **2** and **3**) leads to considerable changes in phase behavior. In compound **2**, a layer structure is observed at room temperature [$d_{\mathrm{L}} = 67.6$ Å, Figure 4(*a*)]. Wide-angle reflection corresponding to an interplanar distance of 10.0 Å and a disordered columnar phase were detected. The latter phase is characterized by five reflections with the ratio of *d*-spacing squares $d_1^2 : d_2^2 : d_3^2 : d_4^2 : d_5^2 : d_6^2 : d_7^2 =$ $= 1:3:4:7:9:13:16$. The measured diameter of the cylinders of the columnar mesophase was $D = 55.6$ Å. Due to the specific packing of azobenzene rings, an unusual electron density distribution inside the columns was revealed, manifesting itself in substantially high relative intensities of reflections 10 and 21. As the column diameter is much smaller than two molecular lengths of **2** ($2 \cdot 37.7$ Å = 75.4 Å), we can assume that the aliphatic tails of dendrons belonging to the neighboring columns, interdigitate considerably. Heating of compound **2** was accompanied by the further improvement of a 2-D hexagonal lattice, with the shift of corresponding reflections to wide angles (the linear coefficient of temperature expansion $\beta = -3.3\times10^{-4}$ K^{-1}). Note

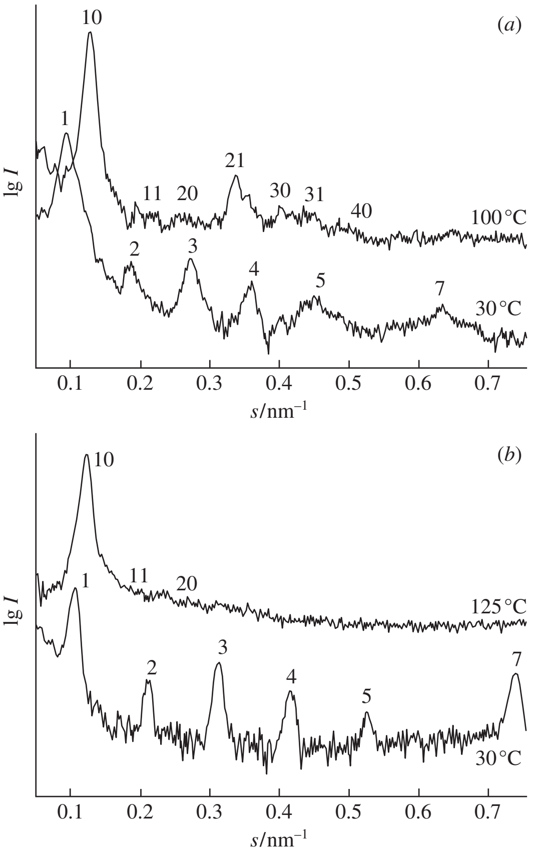

Figure 4 Small-angle X-ray scattering patterns of compounds (*a*) **2** and (*b*) **3** in smectic bilayer (30 °C) and 2-D columnar (100 and 125 °C, respectively).

that the considerable energy of interaction of the aromatic rings of the mesogenic groups leads to the stabilization of the disordered columnar mesophase up to thermolytic destruction.

A comparative analysis of the structure of supramolecular ensembles formed by sodium (**2**) and pyridinium (**3**) *p*-{(*E*)-*p*-[3,4,5-tris(dodecyloxy)benzoyloxy]phenylazo}benzenesulfonate molecules revealed the significant role in phase behavior of material played by the interaction of ionic pairs. The temperature range of the existence of columnar mesophases is considerably narrower in compound **3** compared to that in compound **2**: a transformation of the nascent ordered bilayer structure [d_L = = 59.5 Å, Figure 4(*b*)] occurs at 95 °C. At 120 °C, the small-angle X-ray patterns of compound **3** exhibit three reflections of a 2-D hexagonal columnar mesophase with the cylinder diameter D = 70.9 Å. Isotropization is observed at 200 °C. On cooling, a recovery of the smectic mesophase proceeds only after the sustained annealing in air (>24 h). The structure, however, differs significantly from that of the nascent samples: the interlayer distance after annealing is 72.4 Å. Possible packing modes of the two types of smectic bilayers formed by the dendrons of compound **3** are presented in Figure 5. Apparently, nascent samples possess a chevron structure, in which dendron planes are tilted by an angle of ~40° relative to the layer director, while they are oriented parallel to the layer planes in the annealed samples.

Thus, a comparative analysis of the structure and phase behavior of the synthesized compounds on the basis of symmetrically and asymmetrically substituted benzenesulfonic acids with bulky aromatic focal groups revealed the important role of specific steric and π–π interactions of such groups, determining the characteristic bilayer structure of the smectic mesophase at room temperature.

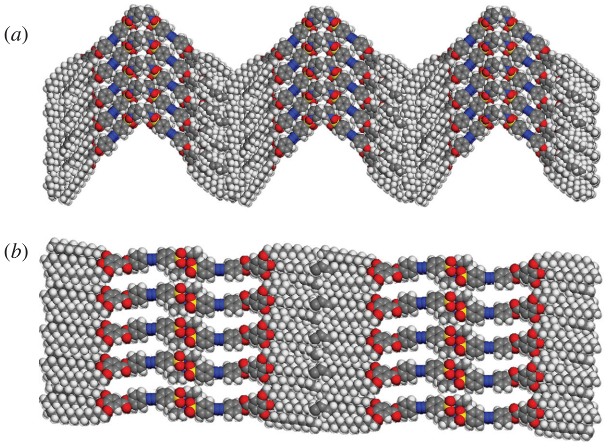

Figure 5 Molecular modeling of supramolecular ensembles formed by the dendrons of compound **3**: (*a*) nascent smectic chevron bilayers and (*b*) smectic mesophase after cooling and sustained annealing.

This work was supported by the Russian Foundation for Basic Research (grant no. 14-03-00975).

References

1 J.-M. Lehn, *Science*, 1985, **227**, 849.
2 J.-M. Lehn, *Angew. Chem., Int. Ed. Engl.*, 1988, **27**, 89.
3 J. N. Izraelachvili, *Intermolecular and Surface Forces*, Academic Press, New York, 1992.
4 S. N. Chvalun, M. A. Shcherbina, I. V. Bykova, J. Blackwell and V. Percec, *Polym. Sci., Ser. A*, 2002, **45**, 1281 (*Vysokomol. Soedin.*, 2002, **45**, 2134).
5 S. N. Chvalun, M. A. Shcherbina, A. N. Yakunin, J. Blackwell and V. Percec, *Polym. Sci., Ser. A*, 2007, **49**, 158 (*Vysokomol. Soedin.*, 2007, **49**, 266).
6 X. Zeng, G. Ungar and M. Impéror-Clerc, *Nature*, 2005, **4**, 562.
7 X. Zeng and G. Ungar, *Soft Matter*, 2005, **1**, 95.
8 G. Ungar, Y. Liu, X. B. Zeng, V. Percec and W.-D. Cho, *Science*, 2003, **299**, 1208.
9 S. N. Chvalun, J. Blackwell, J. D. Cho, Y. K. Kwon, V. Percec and J. A. Heck, *Polymer*, 1998, **39**, 4515.
10 V. Percec, A. E. Dulcey, V. S. K. Balagurusamy, Y. Miura, J. Smidrkal, M. Peterca, S. Nummelin, U. Edlund, S. D. Hudson, P. A. Heiney, H. Duan, S. N. Magonov and S. A. Vinogradov, *Nature*, 2004, **430**, 764.
11 Y. Chen, M. D. Lingwood, M. Goswami, B. E. Kidd, J. J. Hernandez, M. Rosenthal, D. A. Ivanov, J. Perlich, H. Zhang, X. Zhu, M. Möller and L. A. Madsen, *J. Phys. Chem. B*, 2014, **118**, 3207.
12 M. W. Matsen and F. S. Bates, *Macromolecules*, 1996, **29**, 7641.
13 L. Leibler, *Macromolecules*, 1980, **13**, 1602.
14 M. W. Matsen and F. S. Bates, *Macromolecules*, 1996, **29**, 1091.
15 S. N. Chvalun, M. A. Shcherbina, I. V. Bykova, J. Blackwell, V. Percec, Y. K. Kwon and J. D. Cho, *Polym. Sci. Ser. A*, 2001, **43**, 33 (*Vysokomol. Soedin.*, 2001, **43**, 40).
16 A. V. Bakirov, A. N. Yakunin, M. A. Shcherbina, S. N. Chvalun, X. Zhu, U. Beginn and M. Möller, *Nanotechnologies in Russia*, 2010, **5**, 762.
17 M. A. Shcherbina, A. V. Bakirov, A. N. Yakunin, V. Percec, U. Beginn, M. Möller and S. N. Chvalun, *Crystallogr. Rep.*, 2012, **57**, 151 (*Kristallografiya*, 2012, **57**, 195).
18 U. Beginn, L. Yan, S. N. Chvalun, M. A. Scherbina, A. Bakirov and M. Möller, *Liq. Cryst.*, 2008, **35**, 1073.
19 M. A. Shcherbina, A. V. Bakirov, A. N. Yakunin, U. Beginn, L. Yan, M. Möller and S. N. Chvalun, *Soft Matter*, 2014, **10**, 1746.
20 H. Zhang, L. Li, M. Möller, X. Zhu, J. J. H. Rueda, M. Rosenthal and D. A. Ivanov, *Adv. Mater.*, 2013, **25**, 3543.
21 H. Rau and D. Rötger, *Mol. Cryst. Liq. Cryst. Sci. Technol., Sect. A*, 1994, **246**, 143.
22 M. Ogawa, M. Hama and K. Kuroda, *Clay Minerals*, 1999, **34**, 213.
23 M. D. Segarra-Maset, P. W. N. M. van Leeuwen and Z. Freixa, *Eur. J. Inorg. Chem.*, 2010, 2075.
24 X. Zhu, B. Tartsch, U. Beginn and M. Möller, *Chem. Eur. J.*, 2004, **10**, 3871.

Received: 13th May 2014; Com. 14/4383